Journal of Alloys and Compounds, 211/212 (1994) 352–355
JALCOM 025

Mechanical loss and elastic modulus associated with phase transitions of barium titanate ceramics*

B.L. Cheng
Department of Physics, South China University of Technology, Guangzhou 510641 (China)

M. Gabbay** and G. Fantozzi
GEMPPM, URA CNRS 341, INSA Lyon, Bâtiment 502, F-69621 Villeurbanne Cedex (France)

W. Duffy Jr.
Department of Physics, Santa Clara University, Santa Clara, CA 95053 (USA)

Abstract

The internal friction (Q^{-1}) and elastic modulus (E) were measured *vs.* temperature ($100 < T < 450$ K) for rectangular plate specimens of $BaTiO_3$ driven electrostatically in flexural vibration at resonance frequencies between 2 and 4 kHz. The $Q^{-1}(T)$ and $E(T)$ curves exhibit the following three phase transitions in $BaTiO_3$: rhombohedral to orthorhombic (T_{R-O}), orthorhombic to tetragonal (T_{O-T}) and tetragonal to cubic (T_{Curie}). Each phase transition induces either a very narrow internal friction peak or a discontinuous change in Q^{-1} and a very sharp anomaly of the elastic modulus. Moreover, two other internal friction peaks are located below the phase transition temperature. These peaks seem to be associated with the motion of domain walls. The secondary peaks are not observed on undoped ceramics sintered at low temperature. The influence of dopants such as Nb and Co results in the attenuation of internal friction and the smoothing of elastic modulus anomalies.

1. Introduction

Barium titanate ($BaTiO_3$) is a ferroelectric ceramic material used by the electronics industry for various applications (capacitors, non-linear positive temperature coefficient resistors, piezoelectric transducers, etc.). However, pure barium titanate cannot be used because there are four crystal structures (rhombohedral, orthorhombic, tetragonal and cubic) between −100 and 135 °C. Consequently the phase transitions induce large variations in permittivity and dielectric loss. In order to avoid this disadvantage, only doped materials are used. Commonly Nb and Co are added to $BaTiO_3$ in order to stabilize the permittivity and to reduce the dielectric loss. In the literature there are numerous studies on the phase transitions of $BaTiO_3$ from dielectric loss and permittivity measurements [1–6]. However, there are very few papers dealing with the same studies from mechanical loss and/or elastic modulus measurements on $BaTiO_3$ [7–10]. The aim of the present paper is to describe experimental results of mechanical loss and elastic modulus measurements on $BaTiO_3$ ceramics and to discuss the influence of dopants such as Nb and Co on the phase transitions.

2. Specimens and experimental procedures

Three kinds of $BaTiO_3$ ceramics were prepared: 1, undoped material; 2, Nb-doped material with 2.0 or 4.0 at.%; 3, Co-doped material with 0.6 or 1.0 at.%.

The barium titanate powder (Elmic BT 100, 0.7–1.0 μm particle size) was supplied by Rhône-Poulenc. Niobium pentoxide and cobalt carbonate powders were added to the barium titanate powder to form an alcoholic suspension. The suspension was mixed by vibration milling with agate balls for 2 h. The mixture was dried and suitable organic binders were added. After drying and deagglomeration, the powders were pressed uniaxially at 30 MPa to form prismatic bars ($8 \times 8 \times 50$ mm^3) and then pressed hydrostatically at 300 MPa. The compacts were sintered in air for 2 h at 1573 or 1513 K and finally sliced into rectangular plates ($1 \times 5 \times 40$ mm^3).

For internal friction and elastic modulus measurements a sample was supported horizontally at its nodal points by two pairs of fine nickel wires. The sample

*Invited paper.
**Author to whom correspondence should be addressed.

SSDI 0925-8388(93)00025-T

was driven electrostatically in flexural vibration; the vibration amplitude was recorded as a function of frequency. Q^{-1} was calculated from the resonance curve according to [11]

$$Q^{-1} = \frac{\Delta f}{f_r \times 3^{1/2}}$$

where Δf is the width of the resonance curve at half-maximum amplitude and f_r is the resonance frequency. E was calculated according to

$$E = \frac{0.9464 \rho L^4 f_r^2}{d^2}$$

where ρ is the density, L is the length and d is the thickness. $Q^{-1}(T)$ and $E(T)$ were measured from 120 to 430 K at a heating rate of 1 K min^{-1} in vacuum. The frequency of vibration was about 3 kHz and the maximum strain amplitude was 1×10^{-6}.

Scanning electron microscopy (SEM) observations were made on samples polished mechanically and lapped from 6 to 1 μm roughness using diamond paste and etched using 5 vol.% conc. HCl and 0.5 vol.% conc. HF.

3. Experimental results

3.1. Undoped $BaTiO_3$ ceramics

Figure 1 shows the variations of elastic modulus E and internal friction Q^{-1} as a function of temperature T for undoped $BaTiO_3$ ceramic sintered in air at 1573 K for 2 h. The $E(T)$ curve shows three very sharp anomalies A_1 (405 K), A_2 (283 K) and A_3 (179 K) which correspond to the following phase transitions: A_1, tetragonal to cubic; A_2, orthorhombic to tetragonal; A_3, rhombohedral to orthorhombic. These anomalies are associated with three narrow peaks P_1, P_2 and P_3 respectively on the $Q^{-1}(T)$ curve. Moreover, the $Q^{-1}(T)$ curve shows a large peak P_2' (250 K) and a small peak P_3' (160 K).

The results obtained from undoped $BaTiO_3$ sintered at 1513 K in air for 2 h are shown in Fig. 2. The three phase transitions induce similar elastic modulus anomalies (A_1, 399 K; A_2, 280 K; A_3, 185 K) and internal friction peaks (P_1, P_2 and P_3), but the P_2' and P_3' peaks are no longer observed.

3.2. Nb-doped $BaTiO_3$ ceramics

Figures 3 and 4 show the internal friction and elastic modulus curves corresponding to 2.0 and 4.0 at.% Nb-doped $BaTiO_3$. Compared with the results for undoped ceramics, the anomalies A_1, A_2 and A_3 of the $E(T)$ curves are smoothed off: the higher the Nb content is, the higher the smoothing is. For 4.0 at.% Nb content the A_2 anomaly disappears completely; similarly the internal friction peak P_1 (400 K) is reduced, the P_2 peak disappears, while the height of the P_3 (233 K) peak remains stable. The temperature of A_3 is shifted to a higher value (from 225 to 233 K) with increasing Nb content (from 2.0 to 4.0 at.%).

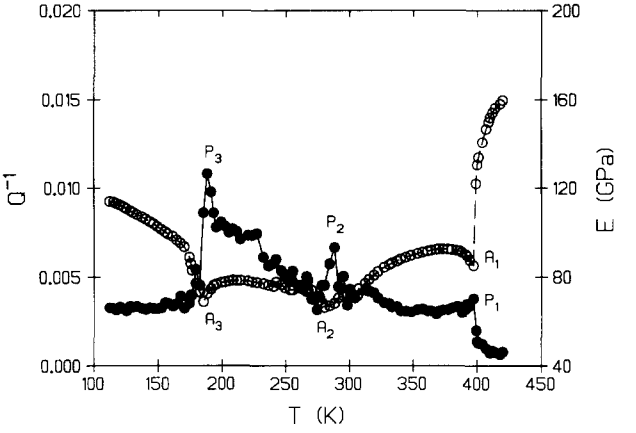

Fig. 2. Variations in E and Q^{-1} *vs.* temperature for undoped $BaTiO_3$ sintered at 1513 K for 2 h.

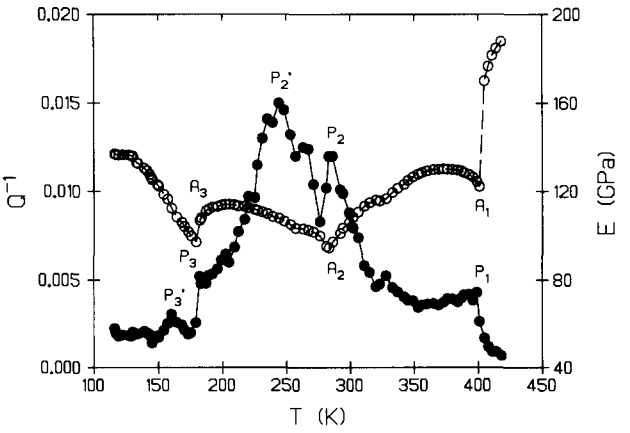

Fig. 1. Variations in E and Q^{-1} *vs.* temperature for undoped $BaTiO_3$ sintered at 1573 K for 2 h.

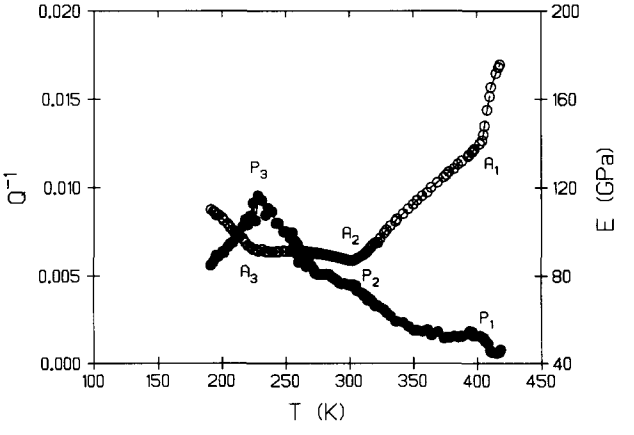

Fig. 3. Variations in E and Q^{-1} *vs.* temperature for $BaTiO_3$ doped with 2.0 at.% Nb and sintered at 1573 K for 2 h.

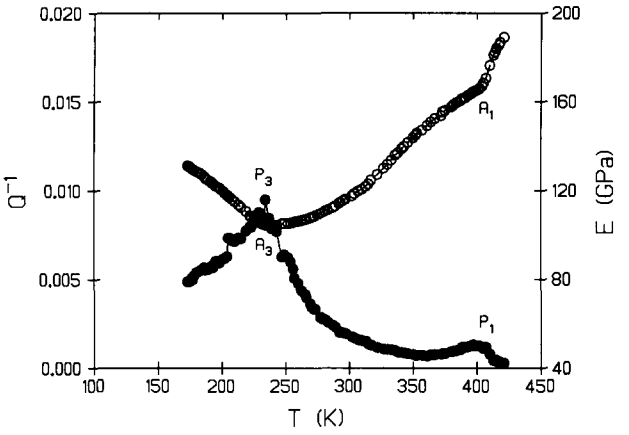

Fig. 4. Variations in E and Q^{-1} *vs.* temperature for $BaTiO_3$ doped with 4.0 at.% Nb and sintered at 1573 K for 2 h.

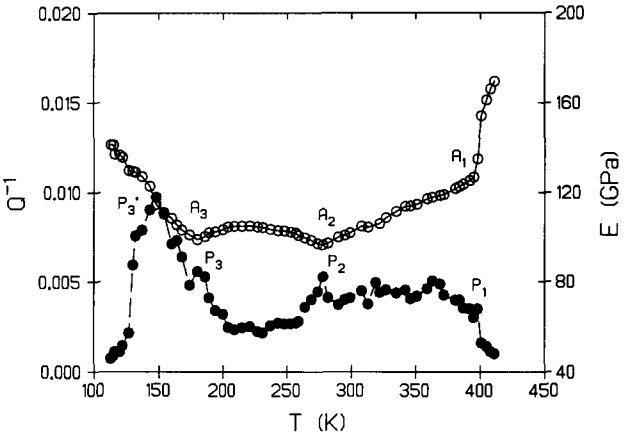

Fig. 5. Variations in E and Q^{-1} *vs.* temperature for $BaTiO_3$ doped with 0.6 at.% Co and sintered at 1573 K for 2 h.

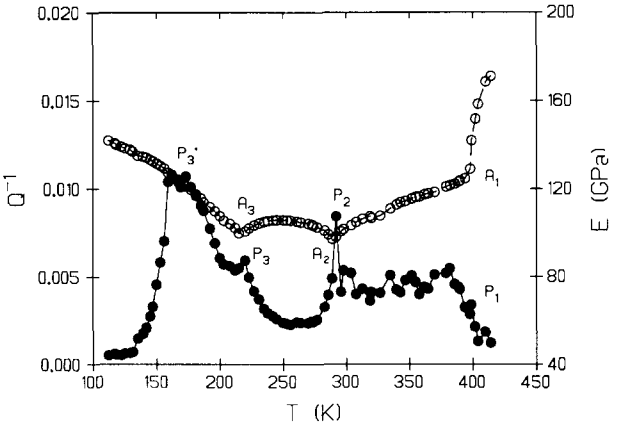

Fig. 6. Variations in E and Q^{-1} *vs.* temperature for $BaTiO_3$ doped with 1.0 at.% Co and sintered at 1573 K for 2 h.

3.3. *Co-doped $BaTiO_3$ ceramics*

Figures 5 and 6 show the internal friction and elastic modulus curves for $BaTiO_3$ doped with 0.6 and 1.0 at.% Co. The anomalies A_1, A_2 and A_3 are located at 398, 278 and 180 K for the 0.6 at.% Co-doped ceramic and at 398, 291 and 215 K for the 1.0 at.% Co-doped ceramic respectively. The anomalies are smoothed off by the Co dopant, but the smoothing is less than that of Nb-doped ceramics. Comparison of the $Q^{-1}(T)$ curves with Fig. 1 shows that (1) the heights of the P_1, P_2 and P_3 peaks are reduced, (2) the internal friction level between the P_1 and P_2 peaks remains unchanged; (3) the internal friction level between the P_2 and P_3 peaks is drastically reduced and (4) the P_3' peak is strongly enhanced.

4. Discussion

4.1. *Influence of grain size*

The three anomaly–peak pairs (A_1, P_1), (A_2, P_2) and (A_3, P_3) can obviously be attributed to the three phase transitions in $BaTiO_3$ ceramics. The P_2' peak, however, is observed only for the ceramic sintered at 1573 K. The structure observed by SEM shows coarse grains (about 50 μm) with numerous domains at 90° (Fig. 7). For the ceramic sintered at 1513 K, Fig. 8 shows a homogeneous structure of fine grains (about 1 μm). Thus the P_2' peak could be attributed to the motion of domain walls in coarse-grained ceramics, while such a motion of domain walls could be limited by grain boundaries in fine-grained ceramics. It is interesting to point out that such a secondary peak has already been observed in ferroelectric lead zirconate titanate (PZT) by Postnikov *et al.* [12] and in ferroelastic LNPP by Chen *et al.* [13]. It is also worthwhile to compare this peak with the secondary peak observed by Sugimoto and Mori [14] in Mn–Cu alloys and attributed to twin boundary relaxation before the phase transition.

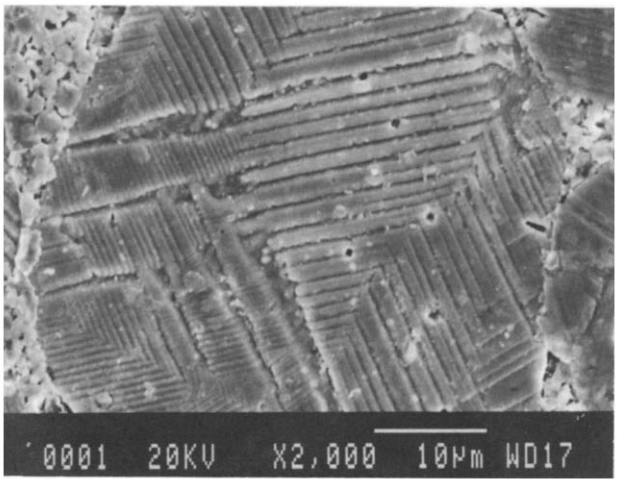

Fig. 7. SEM image of undoped $BaTiO_3$ sintered at 1573 K for 2 h.

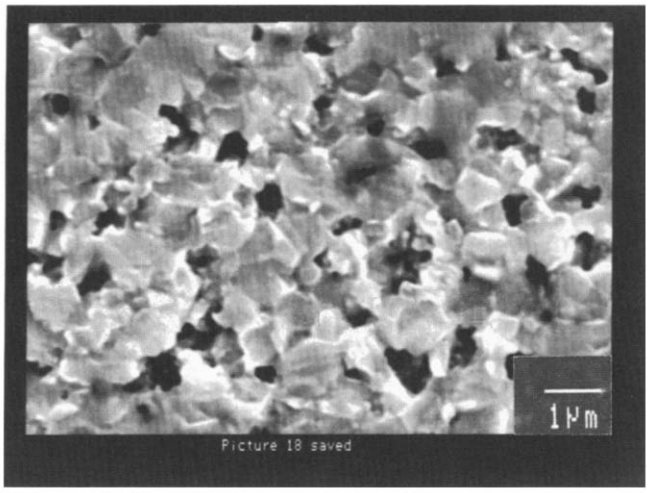

Fig. 8. SEM image of undoped $BaTiO_3$ sintered at 1513 K for 2 h.

4.2. Influence of Nb dopant

SEM observations show that the Nb dopant inhibits grain growth during sintering. The grain size of Nb-doped ceramics is about 1–2 μm. The disappearance of the (A_2, P_2) pair could be attributed to the shift of the Curie point towards low temperatures as shown by Kahn [1]. Such a shift is probably due to the partial intragranular diffusion of Nb which leads to the so-called "core–shell" structure: the grain core remains pure, while the dopant content increases towards the grain boundary. Such a heterogeneous composition inside the grain gives a distribution of the Curie temperature [15]. The shift of the (A_3, P_3) pair towards high temperatures is probably correlated with such a "core–shell" structure.

4.3. Influence of Co dopant

SEM observations show that Co also inhibits grain growth during sintering. The grain size is about 1–2 μm. Ihrig [16] reported that the effect of the Co dopant results in shifts of both T_{Curie} and T_{T-O} towards low temperatures and T_{R-O} towards high temperatures. Thus these results can explain the reduction in temperature range of the orthorhombic phase.

The difference in the valence state of those two dopants (Nb^{5+}, Co^{3+}) can be used to explain the different influences on the internal friction curves. In Co-doped ceramics the large peak P_3' located in the rhombohedral phase could be due to the motion of domain walls.

5. Conclusions

In undoped $BaTiO_3$ ceramic with large grain sizes and large ferroelectric domains, sintered at 1573 K, each phase transition induces a very narrow internal friction peak and a very sharp anomaly of the elastic modulus. Moreover, an internal friction peak exists before each phase transition; such peaks seem to be associated with the motion of domain walls. The influence of dopants such as Nb and Co results in the attenuation of internal friction and the smoothing of elastic modulus anomalies. The Nb dopant reduces the internal friction in the tetragonal phase, while the Co dopant reduces the internal friction in the orthorhombic phase. In order to determine the mechanisms of the P_2' and P_3' peaks, low frequency measurements will be carried out.

Acknowledgments

The authors are very grateful to J. Paletto and M. Taha for specimen preparations, to C. Olagnon for SEM observations and to D. Lavielle and G. Orange for valuable discussions.

References

1 M. Kahn, *J. Am. Ceram. Soc., 54* (1971) 455.
2 D. Lavielle, J. Poumarat, Y. Montardi, P. Bernard and O. Agurre-Charriol, in G. Ziegler and H. Hausner (eds.), *Second Euro-Ceramics, Ausburg, September 1991, Deutsche Keramische Gesellschaft e.V., 3* (1991) 1903.
3 R.F. Blunt and W.F. Love, *Phys. Rev., 76* (1949) 1202.
4 H.C. Graham, N.M. Tallan and K.S. Mazdiyasni, *J. Am. Ceram. Soc., 54* (1971) 548.
5 H.J. Hagemann, *J. Phys. C: Solid State Phys., 11* (1978) 3333.
6 T.S. Fang, H.L. Hsieh and F.S. Shiau, *J. Am. Ceram. Soc., 76* (1993) 1205.
7 T. Ikeda, *J. Phys. Soc. Jpn., 12* (1958) 809.
8 E.J. Huibregtse, W.H. Bessy and M.E. Drougard, *J. Appl. Phys., 30* (1959) 899.
9 A.Yu. Kudzin, L.K. Bunina and O.A. Grzhegorzhevskii, *Sov. Phys. – Solid State, 11* (1970) 1939.
10 A.Yu. Kudzin, E.P. Kashchenko and V.I. Kostrub, *Sov. Phys. – Solid State, 12* (1972) 3162.
11 C. Zener, *Elasticity and Anelasticity of Metals,* University of Chicago Press, Chicago, IL, 2nd edn., 1952, Chap. 6.
12 P.V. Postnikov, V.S. Pavlov, S.A. Gridev and S.K. Turkov, *Sov. Phys. – Solid State, 10* (1968) 1267.
13 X. Chen, Y. Wang, H. Shen, Z. Niu and P.C.W. Fung, in T.S. Kê (ed.), *Proc. ICIFUAS-9, Beijing, July 1989,* International Academic Publishers, Pergamon Press, Oxford, 1989, p. 153.
14 K. Sugimoto and T. Mori, in D. Lenz and K. Lücke (eds.), *Proc. ICIFUAS-5, Aachen, August 1973,* Springer-Verlag, Berlin, 1975, p. 418.
15 D. Hennings and G. Rosenstein, *J. Am. Ceram. Soc., 67* (1984) 249.
16 H. Ihrig, *J. Phys. C: Solid State Phys., 11* (1978) 819.